Coherent Stokes Raman spectroscopy of conduction electron spin flip transitions in $Cd_{1-x}Fe_xTe$: A Van Vleck paramagnet

A. Winter and H. Pascher
Experimentalphysik I, Universität Bayreuth, D-95440 Bayreuth, Germany

H. Krenn
Institut für Experimentalphysik, Karl-Franzens-Universität Graz, A-8010 Graz, Austria

I. Miotkowski and A. K. Ramdas
Department of Physics, Purdue University, West Lafayette, Indiana 47907, USA
(Received 12 September 2007; revised manuscript received 24 June 2008; published 30 July 2008)

The conduction-band spin splitting in $Cd_{1-x}Fe_xTe$ bulk crystals is delineated on the basis of the Raman transitions manifested in coherent Stokes Raman scattering (CSRS). The independence at low temperatures and absence of saturation at high magnetic fields displayed by the Raman shift are characteristic of Van Vleck paramagnetism of Fe^{2+} interacting with *s*-like conduction electrons via the *s-d* exchange interaction. The exchange constant $(N_0\alpha)$ deduced from these experiments is (255 ± 10)meV. When Fe^{2+} concentration (x) exceeds ~0.002 the intrinsic negative *g*-factor of electrons in CdTe is compensated by the positive *s-d* exchange interaction. The separation of the first magnetic excited state Γ_4 lying just above the nonmagnetic Γ_1 ground state, deduced from the analysis of the spin splitting as a function of temperature, is 16 ± 2 cm^{-1}.

DOI: 10.1103/PhysRevB.78.045213 PACS number(s): 78.20.Ls, 78.55.Et, 42.65.Dr, 75.50.Pp

I. INTRODUCTION

Spontaneous, i.e., conventional Raman spectroscopy, has been successfully exploited in the exploration, discovery, and delineation of vibrational, electronic and magnetic excitations in a variety of II–VI ternaries in which the group II cations have been randomly replaced with a member of the 3*d* transition metal ion (TMI).[1,2] Examples of such ternaries, designated as diluted magnetic semiconductors (DMSs), are the Mn-based $Cd_{1-x}Mn_xTe$ and $Cd_{1-x}Mn_xSe$. While Mn ions can be introduced in them with x values as large as 0.77 and 0.55,[2] the majority of the 3*d*-TMIs enter with a significantly smaller x. For example, the maximum x in $Cd_{1-x}Fe_xTe$ and $Cd_{1-x}Fe_xSe$ is ~0.05. One has then to resort to resonance Raman scattering in their studies.[3,4] It is in this context that Coherent Stokes Raman scattering (CSRS)[5,6] offers unique advantages over spontaneous Raman scattering as underscored in Sec. II. In Ref. 5 we applied CSRS to study Raman-electron paramagnetic resonance of Mn^{2+} and spin-flip Raman scattering from donor bound as well as conduction electrons in $Cd_{1-x}Mn_xTe$ bulk crystals and in Ref. 6 we showed that one can employ it effectively in the context of superlattices like CdTe/MnTe.

In the present paper we apply CSRS to investigate spin flip excitation of conduction electrons in $Cd_{1-x}Fe_xTe$, which displays the unique paramagnetism named after Van Vleck.[7]

II. EXPERIMENTAL DETAILS

Coherent Raman scattering

The coherent Raman scattering techniques CARS (coherent anti-Stokes Raman scattering) and CSRS are types of optical four-wave mixing spectroscopy,[8,9] where two laser beams with frequencies ω_L and ω_S are superimposed in a sample and generate radiation with new frequencies: $\omega_{CARS}=2\omega_L-\omega_S$ or $\omega_{CSRS}=2\omega_S-\omega_L(\omega_L>\omega_S)$. The output intensity of the CSRS radiation is proportional to the square of the length of the sample, to a phase factor resulting from the $\boldsymbol{k}$-conservation rule and to the square of the third-order nonlinear susceptibility $\chi^{(3)}$, which contains all the specific properties of the semiconductor material under consideration. Since in most of our cases the sample length is smaller than the coherence length for collinear beams, we used a collinear geometry which is easier to align, than a noncollinear phase matched condition, particularly when the laser frequencies are tuned.

The nonlinear susceptibility $\chi^{(3)}$ exhibits maxima at Raman frequencies whenever $\hbar(\omega_L-\omega_S)$ is equal to the excitation energy of a Raman allowed transition. Furthermore, one-photon resonances may occur, if the "incident" photon energy $\hbar\omega_L$ corresponds to the energy of a real, dipole allowed, electronic transition, e.g., an allowed interband transition. If both Raman and one-photon resonance occur simultaneously, the CSRS intensity will be enhanced by several orders of magnitude yielding "resonant CSRS." To fulfill the polarization selection rules, the incident beams with ω_L and ω_S have to be polarized as the exciting laser and the scattered, say, Stokes radiation in the corresponding spontaneous Raman experiment. In the case of the conduction-band free-electron spin resonance (CSF) two collinear laser beams $(\boldsymbol{k_L}/|\boldsymbol{k_L}|=\boldsymbol{k_S}/|\boldsymbol{k_S}|)$ may be polarized linearly and perpendicular to each other $(\omega_L{:}\boldsymbol{E_L}\perp\boldsymbol{B},\ \omega_S{:}\boldsymbol{E_S}\|\mathbf{B})$ in Voigt configuration $(\boldsymbol{B}\perp\boldsymbol{k})$ to observe spin resonances in a CSRS experiment. CSF satisfies the condition $\hbar(\omega_L-\omega_S)=g\mu_BB_{res}$.

The coherent Raman technique has four main advantages with respect to spontaneous Raman scattering: (i) The spectral resolution is defined by the lasers and not by the instrumental width of a spectrometer. (ii) Small Raman shifts are easier to detect; in our case Raman shifts below 0.5 cm^{-1} can be resolved. (iii) An excellent spatial discrimination

against a luminous background is ensured by the unique directions in which the CSRS signal is emitted, in contrast to the diffuse nature of the unavoidable unshifted, i.e., "parasitical" incident laser radiation in spontaneous Raman scattering. (iv) Due to the short pulses of the *Q*-switched lasers the energy deposited in the sample and thus the sample heating is much lower than in a spontaneous Raman experiment using cw pump lasers.

To excite the coherent Raman spectra, we used two dye lasers (CONTINUUM, TDL 60) which were simultaneously pumped by the second harmonic of a 50 Hz *Q*-switched Nd:YAG laser (CONTINUUM YG 681–50). Using a grating under grazing incidence, one obtains a dye laser linewidth lower than 0.1 cm^{-1} without etalons in the cavity.

In order to fulfill the selection rules for spin-flip Raman resonances in CSRS, the polarization of the radiation of one of the exciting lasers has to be rotated by 90°, which we achieve using a KD^*P Pockels cell in dc operation. The dye laser beams were then made collinear to each other with a calcite crystal and attenuated by several orders of magnitude down to a few microjoules each, before focusing them on the sample kept in the Voigt geometry inside a 7 T superconducting split-coil magnet system, either immersed in superfluid helium pumped down to $T=1.7$ K or held in a helium gas flow at a stabilized temperature using a temperature controller.

Experiments of the present investigation were performed in the temperature range from 1.7 K up to 200 K. The radiation generated by four-wave mixing was collected in forward direction and then focused onto the entrance slit of a 0.85 m double spectrometer, in order to separate the signal from the laser radiation. Note that in CSRS experiments the spectral resolution obtained does not depend primarily on the resolving power of the spectrometer nor is the spectrometer necessary for a determination of the signal wavelength. The CSRS signal is detected with a liquid nitrogen cooled charge coupled device (CCD) camera. Besides a very low dark current of only a few electrons per minute and a maximum quantum efficiency of about 50%, this 512×512 pixel detector chip offers a unique feature when compared to a photomultiplier system: Working without a spectrometer exit slit, a relatively large wave-number range is recorded in one and the same image, e.g., 70 cm^{-1} (at 632 nm) with our apparatus. On this scale, a background due to luminescence or residual stray light is fairly broad in the dispersion direction, whereas the coherent Raman line covers more or less one pixel. Thus even signals having only a small fraction of the mean background intensity can be detected with confidence. For many subsequent laser frequency differences $\Delta\omega=\omega_L-\omega_S$, such images are taken and in this manner the signal intensity at ω_{CSRS} as a function of $\Delta\omega$ is recorded. More specifically, the procedure for discovering a CSRS resonance consists of recording CCD images in the range of ω_{CSRS} for successive values of $(\omega_L-\omega_S)$, with ω_L being held fixed and ω_S tuned (in steps as small as 0.03 cm^{-1} for narrow Raman lines). In order to obtain high CSRS signals with low pump intensities, resonance CSRS conditions were achieved by tuning ω_L close to the energy gap (varying with x) of the sample.

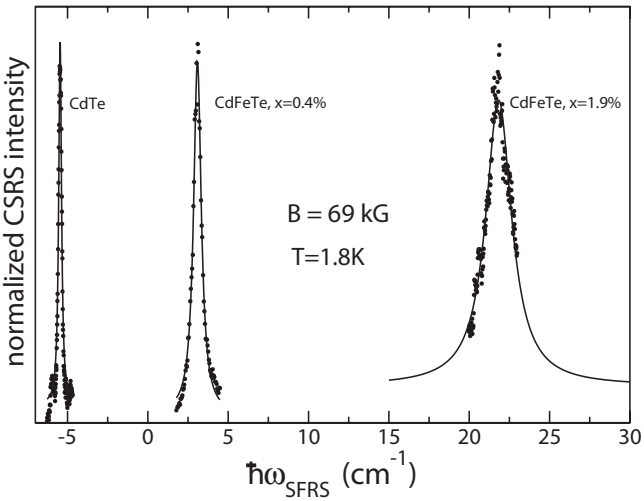

FIG. 1. CSRS spectra at $\hbar\omega_{SFRS}$ of Fe^{2+} in CdTe and $Cd_{1-x}Fe_xTe$ with $x=0.004$ and 0.019. The full lines are fits with Lorentzian line shapes yielding halfwidths of 0.2, 0.6, and 1.9 cm^{-1} for $x=0$, 0.004, and 0.019, respectively.

III. THEORETICAL CONSIDERATIONS

A. Spin-flip Raman scattering from band electrons and electrons bound to effective-mass donors

In this section we consider the so-called spin-flip Raman scattering (SFRS), the Raman signature which has its origin in the spin flip of an electron (either free or donor bound) in a DMS placed in an external magnetic field. The Zeeman splitting is given by

$$\hbar\omega_{SFRS}=\Delta_{CB}=g^*\mu_B B-x\alpha N_0\langle\langle S_z\rangle\rangle. \tag{1}$$

The term $g^*\mu_B B$ describes the intrinsic Zeeman splitting of the conduction electrons in the CdTe host characterized by $g^*=-1.677$ (see Fig. 1) in excellent agreement with -1.676 deduced by Tsoi *et al.*[10] The second term is the exchange energy arising from *s-d* exchange interaction and $\langle\langle S_z\rangle\rangle$ is the thermal and spatial average of the magnetic ion spin projection on the direction of magnetic field. The term $\langle\langle S_z\rangle\rangle$, expressed in terms of the macroscopic magnetization M_m^* associated with the Fe^{2+}, is given by[3]

$$M_m^*=-\frac{\mu_B N_A x}{W(x)}\langle L_z+2s_z\rangle, \tag{2}$$

where $W(x)$ is the molecular weight of the DMS and N_A is the Avogadro's number. Equation (1) can then be rewritten as

$$\hbar\omega_{SFRS}=g^*\mu_B B+\alpha N_0\left(\frac{W(x)}{\mu_B N_A}\right)\left(\frac{\langle S_z\rangle}{\langle L_z+2S_z\rangle}\right)M_m^*. \tag{3}$$

The theoretically calculated value for $\langle L_z+2S_z\rangle/\langle S_z\rangle$ for an isolated Fe^{2+} in $Cd_{1-x}Fe_xTe$ at 1.9 K is 2.29 ± 0.01 (Ref. 11). In order to account for the *d-d* interaction between nearest-neighbor Fe^{2+}, it has been shown in Ref. 11 that

$$\frac{\langle S_z\rangle}{\langle L_z+2S_z\rangle}=\frac{(1-P)\langle S_z\rangle}{P\langle L_z\rangle+(1-P)\langle L_z+2S_z\rangle}, \tag{4}$$

where $P=12\times(1-x)$.

B. Internal level structure of Fe^{2+} in relation to its paramagnetism

The internal electronic level structure of Fe^{2+} in $Cd_{1-x}Fe_xTe$ following a combination of crystal field splitting, spin-orbit and possibly Jahn-Teller effects consists of a nonmagnetic Γ_1 and several magnetic excited states above it. (See Fig. 1 in Tsoi *et al.*)[3] The resulting unique type of magnetic behavior arises from the mixing of the ground state with the magnetic levels lying above, induced by the applied magnetic field **B** with a magnetic moment M_m^* parallel to it at low temperatures; thermal population of the magnetic levels contributes to M_m^* at higher temperatures (see Lu *et al.*[4]). The resulting unique magnetism thus engendered is the Van Vleck paramagnetism. The temperature and magnetic-field dependence of $\hbar\omega_{SFRS}$ follow that of M_m^* in Eq. (3). If one attributes the entire magnetism to the mixing effect and the thermal population to Γ_4, the first magnetic excited state of Fe^{2+} lying at Δ above Γ_1, the temperature dependence of M_m^* for a Van Vleck paramagnet is given by

$$M_m^*(T) = M_0 \cdot \left(1 - \exp\left(-\frac{\Delta}{kT}\right)\right), \tag{5}$$

where M_0 is the magnetization at $T=0$ K. (In Lu *et al.*[4] the mixing with and the thermal population of all the higher magnetic levels are taken into account in the analogous case of $Z_{n-x}Fe_xTe$.)

IV. RESULTS AND DISCUSSION

The CSRS spectra of CdTe and $Cd_{1-x}Fe_xTe$ ($x=0.004$ and $x=0.019$) are displayed in Fig. 1; the line of CdTe exhibits a width of only 0.2 cm^{-1}. The abscissa correspond to the Raman shift observed in CSRS, i.e., $\hbar\omega_{SFRS}$ given by Eq. (1). For a given x and with a temperature low enough and magnetic fields high enough, the contribution of the exchange interaction $x\alpha N_o\langle\langle S_z\rangle\rangle$ equals $g^*\mu_B B$ and reverses the sign of $\hbar\omega_{SFRS}$. For $x=0.004$ and $B=68.5$ kG, this reversal occurs at 20 K whereas for $x=0.019$ it is expected at 160 K, in the temperature range where CSRS becomes too broad to be observed.

The Raman shifts as a function of temperature are displayed in Fig. 2(a) for $x=0.004$ and 0.019 at $B=68.5$ kG, while Fig. 2(b) shows the corresponding magnetizations measured with superconducting quantum interference device (SQUID) magnetometry. One of the unique signatures of Van Vleck paramagnetism, viz., temperature independence of magnetization at low temperatures is unambiguously observed in Fig. 2(a) and verified in the curves in Fig. 2(b). The value of the zero-field separation Δ between Γ_1 and Γ_4 is 16 cm^{-1} (2.0 meV) resulting from fits of Eq. (5) to the CSRS data. Infrared absorption spectra by Slack *et al.*[12] yield 18.6 cm^{-1} (2.31 meV) for very low Fe concentrations, the $\Gamma_1 \rightarrow \Gamma_4$ transition being attributed to a magnetic dipole allowed but electric dipole forbidden transition. This transition has also been directly observed in spontaneous Raman scattering by Tsoi *et al.*[3]

The data displayed in Figs. 2(a) and 2(b) yield $N_0\alpha = (255 \pm 10)$meV and (239 ± 10)meV for $x=0.004$ and 0.019, respectively. The increase in $N_0\alpha$ for the smaller Fe^{2+} concentration can be attributed to the *smaller* number of antiferromagnetically coupled Fe-Fe pairs.[3] We therefore consider $N_0\alpha = (255 \pm 10)$meV as more reliable. The distinctly superior experimental technique of CSRS in comparison to that of spontaneous Raman spectroscopy has thus enabled this measurement for x as low as 0.004 and $N_0\alpha$ higher than 244 meV reported in Ref. 3 for $x=0.009$.

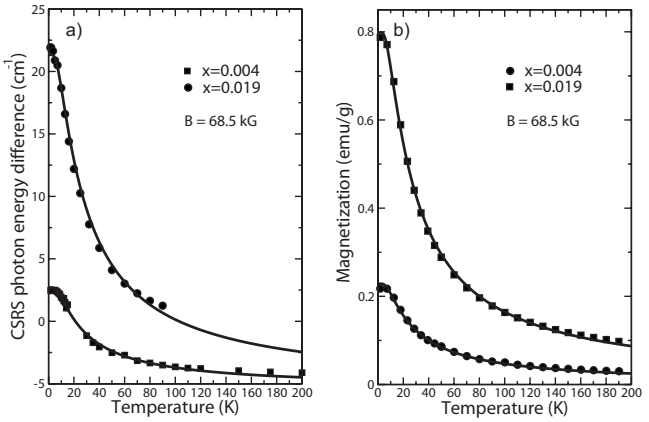

FIG. 2. (a) Conduction-band spin splitting as a function of temperature at 68.5 kG. The experimental values being the spin flip Raman shift measured with CSRS. (b) Magnetization of $Cd_{1-x}Fe_xTe$ measured by SQUID magnetometry as a function of temperature for $x=0.004$ and 0.019. Note: $g^*\mu_B B$ term is omitted in this figure. The solid lines are calculated with Eq. (5) using $\Delta = 16$ cm^{-1}.

The magnetic-field dependences of the CSRS line at $\hbar\omega_{SFRS}$ for $x=0.004$ and 0.019 are displayed in Figs. 3(a) and 3(b), respectively, for several temperatures. The full lines are calculated from Eq. (1) ($g^*=-1.677$, $N_0\alpha=255$ meV) and the magnetization is measured with a SQUID magnetometer. The *s-d* exchange energy $x\alpha N_0\langle\langle S_z\rangle\rangle$ is plotted vs magnetic field in Fig. 4.

Figure 5 shows the linewidth of the CSRS line due to conduction electron spin resonance. The line broadening in CdFeTe is caused by compositional alloy fluctuations and

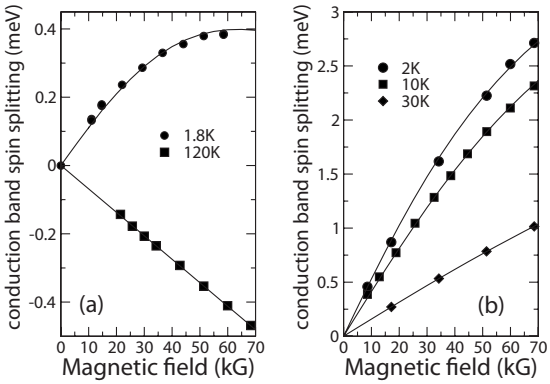

FIG. 3. Spin flip Raman shift measured by CSRS of $Cd_{1-x}Fe_xTe$ as a function of magnetic field for (a) $x=0.004$ at $T=1.8$ K and 120 K, and for (b) $x=0.019$ at $T=2$ K, 10 K, and 30 K. The full lines are fits to experimental data based on Eq. (1) which includes the term $g^*\mu_B B$.

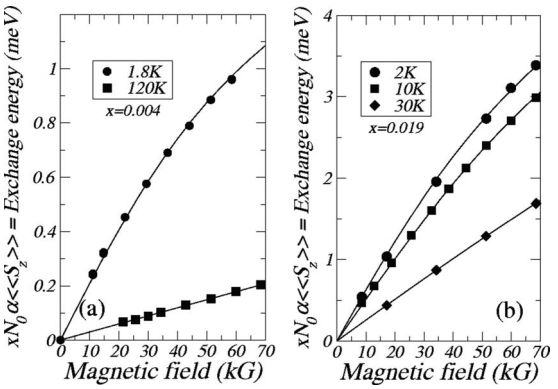

FIG. 4. Exchange energy vs magnetic field at different temperatures for $Cd_{1-x}Fe_xTe$, $x=0.004(a)$ and $x=0.019(b)$. The full lines are fits based on Eq. (1), $g^*\mu_B B$ contribution subtracted.

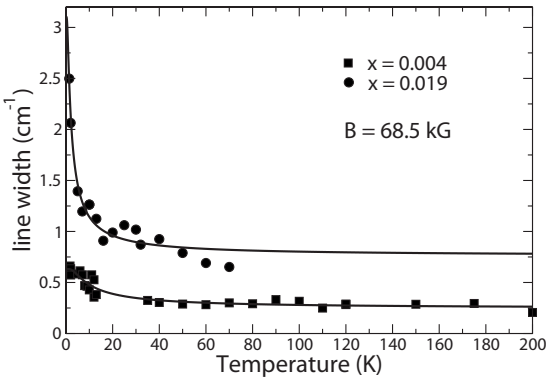

FIG. 5. Halfwidth of the CSRS line as a function of temperature, with the magnetic field $B=68.5$ kG.

hence increases linearly with the *s-d* exchange interaction. Thus the temperature dependence of the linewidth roughly follows the magnetization [Fig. 2(b)]. The flattening at low temperatures, characteristic of a Van Vleck system, is seen in the curve for the 0.4% sample. With the 1.9% sample it occurs for temperatures below 1.8 K, which is not attainable with our cryostat.

In conclusion, Coherent Stokes Raman scattering applied to the Van Vleck paramagnetic system CdFeTe allows a measurement of the conduction-band spin splitting without heating of the samples by strong cw lasers as may occur with spontaneous Raman scattering. The high spectral resolution of the method yields precise data on the linewidth of the spin flip Raman resonance not influenced by instrumental width. The ability of CSRS to observe very small Raman shifts allows one to obtain data very close to the temperature where the spin splitting changes its sign. Although the material parameters in principle are known from spontaneous Raman investigations, the particular advantages of the coherent Raman technique in obtaining higher precision should be underscored.

ACKNOWLEDGMENTS

The authors thank D. Krausse, Bayerisches Geoinstitut, for microprobe analysis. They are also indebted to S. Tsoi and X. Lu for many stimulating discussions and for their help in the preparation of several figures. The authors at Purdue thank the U.S. National Science Foundation (Grants No. DMR 0405082 and 0705793).

[1] A. K. Ramdas and S. Rodriguez, in *Light Scattering in Solids VI*, edited by M. Cardona and G. Güntherodt (Springer, Heidelberg, 1991), pp. 137–206; D. Heiman, in *The Spectroscopy of Semiconductors*, Semiconductors and Semimetals Vol. 36, edited by D. G. Seiler and C. L. Littler (Academic, New York, 1992), pp. 1–83.

[2] *Diluted Magnetic Semiconductors*, edited by J. K. Furdyna and J. Kossut, Semiconductors and Semimetals Vol. 25 (Academic, San Diego, 1988); J. K. Furdyna, J. Appl. Phys. **64**, R29 (1988).

[3] S. Tsoi, I. Miotkowski, S. Rodriguez, A. K. Ramdas, H. Alawadhi, and T. M. Pekarek, Phys. Rev. B **72**, 155207 (2005).

[4] X. Lu, I. Miotkowski, A. K. Ramdas, S. Rodriguez, H. Alawadhi, and T. M. Pekarek, Phys. Rev. B **76**, 035208 (2007).

[5] R. Rupprecht, B. Müller, H. Pascher, I. Miotkowski, and A. K. Ramdas, Phys. Rev. B **58**, 16123 (1998).

[6] R. Rupprecht, B. Müller, H. Pascher, W. Faschinger, W. Sitter, G. Bauer, and A. K. Ramdas, Mater. Sci. Forum **182-184**, 767 (1995).

[7] J. H. Van Vleck, *The Theory of Electric and Magnetic Susceptibilities* (Oxford University Press, London, 1932).

[8] M. D. Levenson and S. S. Kano, *Introduction to Nonlinear Laser Spectroscopy* (Academic, San Diego, 1987).

[9] G. L. Eesley, *Coherent Raman Spectroscopy* (Pergamon, Oxford, 1981).

[10] S. Tsoi, I. Miotkowski, S. Rodriguez, A. K. Ramdas, H. Alawadhi, and T. M. Pekarek, Phys. Rev. B **69**, 035209 (2004).

[11] C. Testelin, C. Rigaux, A. Mycielski, M. Menant, and M. Guillot, Solid State Commun. **78**, 659 (1991).

[12] G. A. Slack, S. Roberts, and J. T. Vallin, Phys. Rev. **187**, 511 (1969).